


# Excited state polarizabilities for CC2 using the resolution-of-the-identity approximation

Nora K. Graf, Daniel H. Friese, Nina O. C. Winter, and Christof Hättig

Citation: The Journal of Chemical Physics **143**, 244108 (2015); doi: 10.1063/1.4937944
View online: http://dx.doi.org/10.1063/1.4937944
View Table of Contents: http://scitation.aip.org/content/aip/journal/jcp/143/24?ver=pdfcov
Published by the AIP Publishing

**Articles you may be interested in**

Two-photon absorption cross sections within equation-of-motion coupled-cluster formalism using resolution-of-the-identity and Cholesky decomposition representations: Theory, implementation, and benchmarks
J. Chem. Phys. **142**, 064118 (2015); 10.1063/1.4907715

A pair natural orbital implementation of the coupled cluster model CC2 for excitation energies
J. Chem. Phys. **139**, 084114 (2013); 10.1063/1.4819071

Large scale polarizability calculations using the approximate coupled cluster model CC2 and MP2 combined with the resolution-of-the-identity approximation
J. Chem. Phys. **136**, 174106 (2012); 10.1063/1.4704788

Analytic gradients for excited states in the coupled-cluster model CC2 employing the resolution-of-the-identity approximation
J. Chem. Phys. **119**, 5021 (2003); 10.1063/1.1597635

Transition moments and excited-state first-order properties in the coupled-cluster model CC2 using the resolution-of-the-identity approximation
J. Chem. Phys. **117**, 6939 (2002); 10.1063/1.1506918




This article is copyrighted as indicated in the article. Reuse of AIP content is subject to the terms at: http://scitation.aip.org/termsconditions. Downloaded to IP: 134.147.252.238 On: Thu, 14 Jan 2016 14:18:42

# Excited state polarizabilities for CC2 using the resolution-of-the-identity approximation

Nora K. Graf,[1,a)] Daniel H. Friese,[2] Nina O. C. Winter,[3] and Christof Hättig[1,b)]
[1]*Lehrstuhl für Theoretische Chemie, Ruhr-Universität Bochum, D-44801 Bochum, Germany*
[2]*Centre for Theoretical and Computational Chemistry CTCC, University of Tromsø, N-9037 Tromsø, Norway*
[3]*Cluster of Excellence RESOLV, Ruhr-Universität Bochum, D-44801 Bochum, Germany*

(Received 13 October 2015; accepted 2 December 2015; published online 23 December 2015)

We report an implementation of static and frequency-dependent excited state polarizabilities for the approximate coupled cluster single and doubles model CC2 as analytic second derivatives of an excited state quasienergy Lagrangian. By including appropriate conditions for the normalization and the phase of the eigenvectors, divergent secular terms are avoided. This leads to response equations in a subspace orthogonal to the unperturbed eigenvectors. It is shown how these projected equations can be solved without storage of the double excitation part of the eigenvectors. By exploiting the resolution-of-the-identity approximation and a numerical Laplace transformation, the quadratic scaling of the main memory demands of RI-CC2 with the system size could be preserved. This enables calculations of excited state polarizabilities for large molecules, e.g., linear polyacenes up to decacene with almost 2500 basis functions on a single compute node within a few days. For a test set of molecules where measurements are available as reference data, we compare the orbital-relaxed and unrelaxed CC2 approaches with experiment to validate its accuracy. The approach can be easily extended to other response methods, in particular CIS($D_\infty$). The latter gives results which, in the orbital-relaxed case, are within a few percent of the CC2 values, while coupled cluster singles results deviate typically by about 20% from orbital-relaxed CC2 and experimental reference data. © *2015 AIP Publishing LLC.* [http://dx.doi.org/10.1063/1.4937944]

## I. INTRODUCTION

Coupled cluster response theory as well as time-dependent density functional theory (TDDFT) are two successful methods for the *ab initio* calculation of excited state properties for large molecules. Excited state properties are important for a detailed understanding of different phenomena, as, for example, the Stark effect or electrochromic properties. Furthermore, excited state properties are crucial for the description of solvatochromic shifts of excitation energies, which is central for the understanding of many photochemical processes, e.g., the excitation process of retinal.[1] TDDFT is applicable to rather large systems but it has with semi-local functionals inherent problems for the description of charge transfer and Rydberg states. On the other hand, coupled cluster methods offer a systematically improvable way for the accurate description of excited state properties, but are computationally demanding. Among the different coupled cluster methods, the approximate coupled-cluster singles-and-doubles model[2] CC2 is an economic approximation to CCSD. It has been shown that its accuracy for adiabatic excitation energies is comparable[3] to that of CCSD, while its computational costs scale with $O(N^5)$ instead of $O(N^6)$ as for CCSD (where $N$ is a measure for the system size).

Excited state polarizabilities can be calculated numerically by application of the finite field approach, in which the molecule is exposed to a small external field. Some of the first calculations[4–6] focused on s-tetrazine, whose excited state polarizability has been experimentally determined by Heitz *et al.*[7] Unfortunately, although the change in the averaged polarizability could be nicely reproduced, there is still a disagreement between the experimental and the calculated results for the individual tensor components.[4–6] Grozema *et al.* calculated excited state polarizabilities of some conjugated molecules with TDDFT, showing that there is an overestimation of the excess polarizability if the molecules become larger.[8] In accordance with these results, Pluta *et al.* pointed out the importance of the correct long-range behavior of the functionals by comparison of TDDFT results with CCSD calculations.[9]

Analytically, the excited state polarizability can be calculated as a double residue of the cubic response function, as done, for example, by Norman *et al.* within the random phase approximation (Hartree-Fock).[10] Jonsson *et al.* extended the implementation to the multi-configurational Hartree-Fock (MCSCF) level and compared the results with linear response calculations of multireference calculations for the excited state.[11,12] Jansik *et al.* implemented the double residue of the cubic response function for TDDFT.[13] Analytical second derivatives in the framework of equation of motion coupled cluster for excited states were discussed by Stanton and Gauss.[14]

a)Author to whom correspondence should be addressed. Electronic mail: nora.graf@rub.de
b)christof.haettig@rub.de

 © 2015 AIP Publishing LLC

This article is copyrighted as indicated in the article. Reuse of AIP content is subject to the terms at: http://scitation.aip.org/termsconditions. Downloaded to IP: 134.147.252.238 On: Thu, 14 Jan 2016 14:18:42

The analytic response approach also allows to compute frequency-dependent polarizabilities. A computational disadvantage has, however, been that the expressions initially obtained from the double residue of the cubic response function contain terms which diverge in the static limit but mutually cancel each other, which leads to numerical instabilities in computations.[10] For most response methods, the double residue of the cubic response function is equivalent to the second derivative of the excitation energy, as, e.g., shown for coupled cluster response theory in Ref. 15. This allows to obtain excited state properties as derivatives of an excited state quasienergy Lagrangian and leads to expressions which do not contain secular divergent terms and are thus numerically stable in the limit of a static perturbation.[15] First coupled cluster response studies were presented for benzene and pyrimidine with CCS, CC2, and CCSD.[6,16] A detailed study of the basis set dependence of excited state polarizabilities for benzene was presented in Ref. 16.

A bottleneck of the CC2 implementation reported in Ref. 6 is the calculation of the four-index electron repulsion integrals (ERIs) in the molecular orbital (MO) basis, which leads to high computational costs as well as storage bottlenecks and limits applications to small molecules. In the framework of the resolution-of-the-identity (RI) approximation, the transformation and storage of four-index intermediates is avoided.[17–19] Only $O(\mathcal{N}^2)$-scaling intermediates have to be kept in main memory and only $O(\mathcal{N}^3)$-scaling intermediates need to be stored on disk. This leads to a considerable reduction of CPU and wall timings and removes the storage bottlenecks[20] and turns CC2 response theory into a valuable alternative to TDDFT for many applications.

In the current paper, we report an extension of RI-CC2 to second-order properties of excited states implemented as orbital-unrelaxed and, for the static limit, as orbital-relaxed derivatives. The latter is a first step for the implementation of analytical force constants for excited states. In Sec. IV, we demonstrate the computational performance of the implementation for systems with up to almost 2500 basis functions and compare in the static limit for a set of organic molecules the results obtained with orbital-unrelaxed CCS and CC2 with orbital-relaxed derivatives for these methods and the CIS($D_\infty$) approximation.

## II. THEORY AND IMPLEMENTATION

### A. The Lagrangian for excited states

The starting point for the calculation of molecular second-order properties for an excited state $f$ with CC2 is the Lagrange function for its total energy. In the orbital-relaxed case, it is given by

$$\begin{aligned}\mathcal{L}^{\mathrm{CC},rel,f} = E_{\mathrm{CC}} &+ \sum_{\mu} \bar{t}^f_\mu \Omega_\mu + \sum_{\mu\nu} L^f_\mu A_{\mu\nu} R^f_\nu + \sum_{\mu_0} \bar{\kappa}^f_{\mu_0} F_{\mu_0} \\ &+ \bar{\omega}^f \Big(1 - \sum_{\mu} L^f_\mu R^f_\mu\Big) \\ &+ \bar{\lambda}^f \Big(\sum_{\mu} L^f_\mu R^{f,(0)}_\mu - \sum_{\mu} L^{f,(0)}_\mu R^f_\mu\Big). \end{aligned} \tag{1}$$

This expression is the same as given in Refs. 21 and 22 except for the last term, which together with the second last term determines uniquely the phase and normalization of the left and right eigenvectors $L^f$ and $R^f$ of the Jacobian $\mathbf{A}$ by coupling them to the eigenvectors $R^{f,(0)}$ and $L^{f,(0)}$ in the unperturbed limit which serves as a reference point. The two constraints prevent together divergent secular contributions that appear in the equations for the derivatives of the eigenvectors.[15]

In the above equation, the energy of the molecule in its electronic ground state is denoted by $E_{\mathrm{CC}}$ and defined as

$$E_{\mathrm{CC}} = \langle \mathrm{HF}|\tilde{\hat{H}} + [\tilde{\hat{H}}, \hat{T}_2]|\mathrm{HF}\rangle, \tag{2}$$

where $|\mathrm{HF}\rangle$ denotes the Hartree-Fock reference function. The singles and doubles cluster operators are given by $\hat{T}_1 = \sum_{\mu_1} t_{\mu_1} \hat{\tau}_{\mu_1}$ and $\hat{T}_2 = \sum_{\mu_2} t_{\mu_2} \hat{\tau}_{\mu_2}$ with the cluster amplitudes $t_{\mu_1}$ and $t_{\mu_2}$ and the single and double excitation operators $\hat{\tau}_{\mu_1}$ and $\hat{\tau}_{\mu_2}$.[23] With $\tilde{\hat{H}}$ we denote a Hamiltonian which is similarity-transformed with $e^{\hat{T}_1}$ as $\tilde{\hat{H}} = e^{-\hat{T}_1} \hat{H} e^{\hat{T}_1}$.

The third term in the excited state Lagrangian yields the excitation energy $\omega^f = \sum_{\mu\nu} L^f_\mu A_{\mu\nu} R^f_\nu$, so that the sum of the first and third term is the total energy of the excited state. The Jacobian matrix $\mathbf{A}$ is defined as the derivative of the vector function $\Omega_\mu$ *(vide infra)* with respect to the cluster amplitudes,

$$A_{\mu\nu} = \frac{\partial \Omega_\mu}{\partial t_\nu}. \tag{3}$$

During this work, we will focus on perturbations which do not change the atomic orbital (AO) basis and can be described by one-electron operators. In the orbital-relaxed case, the second quantized Hamiltonian in the presence of a perturbation with a strength $\epsilon$ can then be expressed in the MO basis of the unperturbed system as

$$\hat{H}(\epsilon) = e^{-\hat{\kappa}} \hat{H}^{(0)} e^{\hat{\kappa}} + e^{-\hat{\kappa}} \hat{V}(\epsilon) e^{\hat{\kappa}}, \tag{4}$$

where $\hat{H}^{(0)}$ describes the unperturbed system and $\hat{V}(\epsilon) = \sum_x \epsilon_x \hat{h}^x$ the perturbation. $\hat{\kappa} = \sum_{\mu_0} \kappa_{\mu_0} (\hat{E}_{\mu_0} - \hat{E}^\dagger_{\mu_0})$ is the orbital rotation operator and $\hat{E}_{\mu_0}$ are the usual spin-free one-particle operators $\hat{E}_{pq} = \hat{a}^\dagger_{p\alpha} \hat{a}_{q\alpha} + \hat{a}^\dagger_{p\beta} \hat{a}_{q\beta}$. With $\mu_0$ we denote the orbital pairs $pq$ for which the Fock matrix elements $F_{\mu_0}$ are required to vanish. This constraint is implemented by the fourth term in the Lagrange function, Eq. (1), and $\bar{\kappa}^f_{\mu_0}$ are the corresponding orbital-rotation Lagrange multipliers for the excited state. In the orbital-unrelaxed case, the coupled cluster wave function is expanded in the orbitals of the unperturbed system, i.e., $\kappa_{\mu_0}$ is kept equal to zero and the contribution $\sum_{\mu_0} \bar{\kappa}^f_{\mu_0} F_{\mu_0}$ is not included in the Lagrange function.

The second term of the Lagrange function accounts for the cluster amplitude equations. The singles equations are given by

$$\Omega_{\mu_1} = \langle \mu_1|\tilde{\hat{H}} + [\tilde{\hat{H}}, \hat{T}_2]|\mathrm{HF}\rangle = 0. \tag{5}$$

For CC2, the doubles equations differ slightly between the orbital-relaxed and unrelaxed case.[2] In the relaxed case they are given by

$$\Omega^{rel}_{\mu_2} = \langle \mu_2|\tilde{\hat{H}} + [\hat{F}, \hat{T}_2]|\mathrm{HF}\rangle = 0, \tag{6}$$

where the Fock operator $\hat{F}$ includes the perturbations. In the unrelaxed case, $\hat{F}$ is replaced[2] by a sum of the unperturbed

This article is copyrighted as indicated in the article. Reuse of AIP content is subject to the terms at: http://scitation.aip.org/termsconditions. Downloaded to IP: 134.147.252.238 On: Thu, 14 Jan 2016 14:18:42

Fock operator $\hat{F}^{(0)}$ and the similarity-transformed perturbation $\tilde{\hat{V}} = e^{-\hat{T}_1}\hat{V}e^{\hat{T}_1}$,

$$\Omega^{ur}_{\mu_2} = \langle \mu_2|\tilde{\hat{H}} + [\hat{F}^{(0)} + \tilde{\hat{V}}, \hat{T}_2]|\mathrm{HF}\rangle = 0. \tag{7}$$

In the following, we will mainly focus on the static orbital-relaxed case. The expression for the unrelaxed case can be obtained from the orbital-relaxed expressions by straightforward simplifications. The extensions for oscillating time-dependent perturbations are obtained by replacing the Hamiltonian by $\hat{H}(\epsilon) - i\frac{d}{dt}$ in all contributions to the Lagrangian, Eq. (1), where $\frac{d}{dt}$ is the time-derivative operator.

The excited state polarizability is obtained as second derivative of the excited state Lagrangian with respect to the strengths of external electric fields. To simplify the expressions obtained by a straightforward differentiation, one can exploit Wigners $2n+1$ rule for the wave function parameters and the stronger $2n+2$ rule for the Lagrange multipliers.[21,24] Here the $2n+1$ rule is used for the cluster amplitudes and the right eigenvectors and the $2n+2$ rule for the Lagrange multipliers and the left eigenvectors. Furthermore, we exploit that the Lagrange multipliers $\bar{\omega}^f$ and $\bar{\lambda}^f$ do not contribute to the second derivative of the energy.[25] We can summarize the expression for second derivatives as follows:

$$\begin{aligned}\left(\frac{d\mathcal{L}^{CC,f,rel}}{d\epsilon_x d\epsilon_y}\right)_{\epsilon=0} &= \langle \hat{J}^{xy}\rangle^{ex} + \hat{P}^{xy}\sum_{pq} D^{F,ex,y}_{pq} F^x_{pq} \\ &+ \hat{P}^{xy}\tfrac{1}{2}\sum_{pqrs} \hat{d}^{nsep,ex,y}_{pqrs}(\hat{pq|rs})^x \\ &+ \sum_{\mu\nu} F^{ex}_{\mu\nu} t^x_\mu t^y_\nu + \hat{P}^{xy}\sum_{\mu\nu\kappa} L^{f,(0)}_\mu B_{\mu\nu\kappa} t^x_\kappa R^{f,y}_\nu .\end{aligned} \tag{8}$$

In the last equation, $\langle \hat{J}^{xy}\rangle^{ex}$ is the expectation value of the effective second-order Hamiltonian,[26]

$$\hat{J}^{xy} = \hat{P}^{xy}\left[\hat{\kappa}^x, \left(\hat{h}^y + \tfrac{1}{2}[\hat{\kappa}^y, \hat{H}]\right)\right], \tag{9}$$

evaluated with the density for the excited state. The operator $\hat{P}^{xy}$ used in Eqs. (8) and (9) symmetrizes with respect to the perturbations $x$ and $y$ according to $\hat{P}^{xy}f(x,y) = f(x,y) + f(y,x)$.

The one-electron densities $D^{F,ex,y}_{pq}$ are contracted with first derivatives of the Fock matrix $F^x_{pq}$ and the non-separable two-electron densities $\hat{d}^{nsep,ex,y}_{pqrs}$ with first derivatives of the electron repulsion integrals $(\hat{pq|rs})^x$ for the similarity-transformed Hamiltonian $\tilde{\hat{H}}$. In the unperturbed limit, the ERIs for $\tilde{\hat{H}}$ are obtained from AO integrals as[27]

$$(\hat{pq|rs}) = \sum_{\mu\nu\kappa\lambda} \Lambda^p_{\mu p}\Lambda^h_{\nu q}\Lambda^p_{\nu r}\Lambda^h_{\lambda s}(\mu\nu|\kappa\lambda), \tag{10}$$

with $\Lambda^p = \mathbf{C}(\mathbf{1} - \mathbf{t}_1^T)$ and $\Lambda^h = \mathbf{C}(\mathbf{1} + \mathbf{t}_1)$, where $\mathbf{C}$ are the coefficients of the HF orbitals.

The last two terms in Eq. (8) collect contributions which are bilinear in the derivatives of the cluster amplitudes and the right eigenvector. $F^{ex}_{\mu\nu}$ and $B_{\mu\nu\kappa}$ are defined as

$$F^{ex}_{\mu\nu} = \left(\frac{\partial \mathcal{L}^{CC,f,rel}}{\partial t_\mu \partial t_\nu}\right)_{\epsilon=0} \tag{11}$$

and

$$B_{\mu\nu\kappa} = \left(\frac{\partial A_{\mu\nu}}{\partial t_\kappa}\right)_{\epsilon=0}. \tag{12}$$

In the orbital-unrelaxed case, all contributions depending on $\bar{\kappa}^f$ and the derivatives $\kappa^x$ vanish. Furthermore, some differences arise in the expressions for the densities and in the right-hand-side vectors of the response equations for $t^x$ and $R^{f,x}$ due to the different form of the doubles equations, Eqs. (6) and (7) (*vide infra*).

While the linear response function of the orbital-unrelaxed approach contains only one set of poles (the coupled cluster poles), the linear response function of the orbital-relaxed approach contains Hartree-Fock and coupled cluster poles, due to its two step nature, which is problematic for the calculation of frequency-dependent properties.[21,28] However, for the frequency-independent case, both approaches are valuable options and previous studies for the ground state polarizability have shown that the orbital-relaxed approach gives often better results.[28,29]

The code can be easily adapted to the CIS($D_\infty$) and ADC(2) methods:[30,31] In CIS($D_\infty$) the ground-state CC2 cluster amplitudes are replaced by the first-order amplitudes $t^{(1)}$ obtained by Møller-Plesset perturbation theory.[3] If the Brillouin condition is fulfilled, the singles cluster amplitudes $t_S$, their derivatives $t^x_S$, and the singles Lagrange multipliers $\bar{t}^f_S$ vanish[3] and the solution of the corresponding equation can be omitted. Since our code uses a partitioned doubles amplitude-direct strategy, this leads automatically to the right expressions for the doubles vectors. Although ten equations with iterative $O(N^5)$-scaling costs need to be solved for the calculation of a full polarizability tensor at the CC2 level, only five such equations need to be solved for CIS($D_\infty$): the left and right eigenvalue equations and three response equations for the first derivatives of the right eigenvectors. For ADC(2), the secular matrix is just the Hermitian part of the secular matrix for CIS($D_\infty$),[3,31]

$$\mathbf{A}^{\mathrm{ADC(2)}} = \frac{1}{2}\left(\mathbf{A}^{\mathrm{CIS}(D_\infty)} + (\mathbf{A}^{\mathrm{CIS}(D_\infty)})^\dagger\right). \tag{13}$$

This difference can be accounted for by minor modifications in the equations for the first derivative of the right eigenvectors and the densities since the above symmetrization affects only one term in the single/singles block of $\mathbf{A}^{\mathrm{CIS}(D_\infty)}$. Because of the Hermitian secular matrix, the left eigenvectors become identical with the right eigenvectors, so that for the calculation of a full polarizability tensor only four equations with iterative $O(N^5)$-scaling costs need to be solved: one eigenvalue problem and three response equations for the first derivatives of the eigenvectors.

### B. Response equations for the right eigenvectors

The first-order response of the right eigenvectors $R^{f,x}$ is determined by the equation[6,15]

$$\mathbf{Q}^f(\mathbf{A} - \omega\mathbf{1})\mathbf{Q}^f R^{f,x} = -\tilde{\xi}^{f,x} \tag{14}$$

with the right hand side vector $\tilde{\xi}^{f,x} = \mathbf{Q}^f\xi^{f,x}$, where

$$\xi^{f,x} = (\mathbf{A}^x + \mathbf{B}t^x)R^{f,(0)}, \tag{15}$$

This article is copyrighted as indicated in the article. Reuse of AIP content is subject to the terms at: http://scitation.aip.org/termsconditions. Downloaded to IP: 134.147.252.238 On: Thu, 14 Jan 2016 14:18:42

and the constraint $L^{f,(0)}R^{f,x} = 0$. In the last equation, $\mathbf{A}^x$ is a Jacobi matrix evaluated with the first derivatives of the MO integrals. The frequency $\omega$ in Eq. (14) is the sum of the excitation energy $\omega^f$ and the frequency of the perturbation $\omega_x$. The operator $\mathbf{Q}^f$ projects onto the orthogonal complement to the unperturbed eigenvectors and is defined as

$$\mathbf{Q}^f = (\mathbf{1} - R^{f,(0)} \otimes L^{f,(0)}). \tag{16}$$

Eq. (14) can be solved either in a subspace orthogonal to $L^{f,(0)}$ with the projected Jacobian $\mathbf{Q}^f\mathbf{A}\mathbf{Q}^f$ or in the full space using the orthogonality condition as constraint. However, an important feature of CC2 is the diagonal structure of the doubles-doubles block of the Jacobian $\mathbf{A}$, which is exploited in RI-CC2 to avoid the storage of $\mathcal{N}^4$-scaling quantities. It allows to partition[20] the eigenvalue problem for $\mathbf{A}$ and the response equations for the cluster amplitudes[29] to effective equations in the single excitation subspace. This technique cannot be applied directly to the projected matrix in Eq. (14). Therefore, we solve instead the linear equation with the unprojected matrix and the constraint that the solution vector is orthogonal to $L^{f,(0)}$. The singles part of the solution vector must fulfill

$$(\mathbf{A}^{eff}_{SS} - \omega\mathbf{1}_{SS})R^{f,x}_S = -\tilde{\xi}^{eff,f,x}_S, \tag{17}$$

with the effective Jacobi matrix defined as[20]

$$\mathbf{A}^{eff}_{SS} = \mathbf{A}_{SS} - \mathbf{A}_{SD}(\mathbf{A}_{DD} - \omega\mathbf{1}_{DD})^{-1}\mathbf{A}_{DS}. \tag{18}$$

Indices $S$ and $D$ denote the singles and doubles parts of the vector space, respectively. The effective RHS vector is given by

$$\tilde{\xi}^{eff,f,x}_S = \xi^{f,x}_S - \mathbf{A}_{SD}(\mathbf{A}_{DD} - \omega\mathbf{1}_{DD})^{-1}\xi^{f,x}_D - \bar{x}^f S^f_S, \tag{19}$$

with the intermediates $\bar{x}^f$ and $S^f_S$ defined as

$$\bar{x}^f = L^{f,(0)}_S\xi^{f,x}_S + L^{f,(0)}_D\xi^{f,x}_D \tag{20}$$

and

$$S^f_S = R^{f,(0)}_S - \mathbf{A}_{SD}(\mathbf{A}_{DD} - \omega\mathbf{1}_{DD})^{-1}R^{f,(0)}_D. \tag{21}$$

They account for the projection of the RHS vector in Eq. (14). The constraint that $R^{f,x}$ has to be orthogonal to $L^{f,(0)}$ can be written as

$$L^{f,(0)}_S R^{f,x}_S - L^{f,(0)}_D(\mathbf{A}_{DD} - \omega\mathbf{1}_{DD})^{-1}(\tilde{\xi}^{f,x}_D + \mathbf{A}_{DS}R^{f,x}_S) = 0. \tag{22}$$

To avoid the storage of doubles intermediates, this condition is cast into the form

$$\bar{S}^f_S R^{f,x}_S = \bar{s}^f \tag{23}$$

with the intermediates

$$\bar{S}^f_S = L^{f,(0)}_S - L^{f,(0)}_D(\mathbf{A}_{DD} - \omega\mathbf{1}_{DD})^{-1}\mathbf{A}_{DS}, \tag{24}$$

$$\bar{s}^f = L^{f,(0)}_D(\mathbf{A}_{DD} - \omega 1_{DD})^{-1}(\xi^{f,x}_D - \bar{x}^f R^{f,(0)}_D). \tag{25}$$

The singles vector $R^{f,x}_S$ is determined by minimizing the residuals of Eqs. (17) and (23) simultaneously. This is numerically stable for perturbations with a finite frequency $\omega_x$ and in the static limit when $\omega = \omega^f$. After the equations for the singles part have been solved, the doubles part can be calculated whenever needed as

$$R^{f,x}_D = -(\mathbf{A}_{DD} - \omega\mathbf{1}_{DD})^{-1}(\xi^{f,x}_D - \bar{x}^f R^{f,(0)}_D + \mathbf{A}_{DS}R^{f,x}_S). \tag{26}$$

Detailed working expressions for the RHS vector $\xi^{f,x}_D$ are given in the supplementary material.[25] As the doubles part of the cluster amplitudes,[20] their derivatives,[29] Lagrange multipliers,[32] and the eigenvectors,[20] also $R^{f,x}_D$ is calculated only when needed on-the-fly and is immediately contracted with left eigenvectors or three-index integrals. This allows to restrict the scaling of the main memory usage with the system size to $O(\mathcal{N}^2)$ and the scaling of disc space usage to $O(\mathcal{N}^3)$.

### C. Evaluation of the unrelaxed one-electron densities

For the one-electron densities $D^{F,ex,y}$, we have to evaluate contributions like $\sum_{ijc} L^{f,(0)}_{aicj}R^{f,x}_{bicj}$, where doubles left eigenvectors are contracted with the doubles of a derivative of the right eigenvectors. Here and in the following, $a, b, c, \ldots$ denote virtual and $i, j, k, \ldots$ occupied MOs. In the RI approximation, four-index ERIs are evaluated as

$$(pq|rs)^{RI} = \sum_Q B^Q_{pq}B^Q_{rs} \tag{27}$$

with

$$B^Q_{pq} = \sum_{P\alpha\beta} C_{\alpha p}C_{\beta q}(\alpha\beta|P)[\mathbf{V}^{-1/2}]_{PQ}, \tag{28}$$

where $(\alpha\beta|P)$ are three-index and $V_{PQ} = (P|Q)$ two-index ERIs. As demonstrated in Ref. 32, the RI approximation is sufficient to implement the one-electron densities that depend only on zeroth-order cluster amplitudes, Lagrange multiplier, and eigenvectors, efficiently with $O(\mathcal{N}^2)$-scaling main memory demands. This is, however, no longer the case for densities that depend on derivatives of eigenvectors or cluster amplitudes. The on-the-fly construction of $R^{f,x}_{aibj}$ for a pair of occupied orbitals $i$, $j$ requires the elements of the unperturbed eigenvector for all pairs $i$, $k$ and $k$, $j$ with any active occupied orbital $k$,

$$\begin{aligned} R^{f,x}_{aibj} = {} & \frac{1}{\Delta\epsilon_{aibj} - \omega} \\ & \times \hat{P}^{ij}_{ab}\Big(\sum_Q \bar{B}^{Q,f,x}_{ai}\hat{B}^Q_{bj} + \sum_Q \bar{B}^Q_{ai}[R^f](\bar{B}^Q_{bj}[t^x] + \hat{B}^{Q,x}_{bj}) \\ & + \sum_c R^{f,(0)}_{aicj}F^x_{bc} - \sum_k R^{f,(0)}_{aibk}F^x_{kj} - \bar{x}^f R^{f,(0)}_{aibj}\Big). \end{aligned} \tag{29}$$

In the last equation, $F^x_{pq}$ are the derivatives of the Fock matrix elements and $\Delta\epsilon_{aibj} = \epsilon_a - \epsilon_i + \epsilon_b - \epsilon_j$. The operator $\hat{P}^{pq}_{rs}$ symmetrizes its operand according to $\hat{P}^{pq}_{rs}f_{pqrs} = f_{pqrs} + f_{rspq}$. The definitions of the different three-index intermediates are given in the supplementary material.[25] To preserve the $O(\mathcal{N}^2)$-scaling main memory demands, we follow the strategy used in Ref. 29 for densities that depend on derivatives of the cluster amplitudes and use a numerical Laplace transformation of the orbital energy denominators[33]

This article is copyrighted as indicated in the article. Reuse of AIP content is subject to the terms at: http://scitation.aip.org/termsconditions. Downloaded to IP: 134.147.252.238 On: Thu, 14 Jan 2016 14:18:42

in the expression for $R^{f,(0)}_{aibj}$,

$$\frac{1}{\epsilon_a - \epsilon_i + \epsilon_b - \epsilon_j - \omega} = \int_0^\infty e^{-(\epsilon_a-\epsilon_i+\epsilon_b-\epsilon_j-\omega)\theta} d\theta \approx \sum_m^{N_m} w_m e^{-(\epsilon_a-\epsilon_i)\theta_m} e^{-(\epsilon_b-\epsilon_j-\omega)\theta_m}. \tag{30}$$

$N_m$ is the number of grid points $\theta_m$ and $w_m$ the integration weights. Within this approximation, the doubles part of the eigenvectors can then be expressed as

$$R^{f,(0)}_{aibj} = -\hat{P}^{ab}_{ij} \sum_{Qm} w_m \hat{K}^{Q,m}_{ai} \bar{K}^{Qm}_{bj}, \tag{31}$$

and the doubles part of their first derivatives can be calculated for a given pair $i, j$ with $O(N^2)$-scaling memory demands,

$$R^{f,x}_{aibj} = \frac{1}{\Delta\epsilon_{aibj} - \omega} \hat{P}^{ij}_{ab} \Big( \sum_Q \bar{\bar{B}}^{Q,f,x}_{ai} \hat{B}^Q_{bj} + \sum_Q \bar{B}^Q_{ai}[R^f](\bar{B}^Q_{bj}[t^x] + \hat{B}^{Q,x}_{bj}) + \sum_{Qm} w_m \hat{K}^{Q,m}_{ai} \bar{\bar{K}}^{Q,m,x}_{bj} + \sum_{Qm} w_m \bar{K}^{Q,m}_{ai} \bar{K}^{Q,m,x}_{bj} - \frac{\bar{x}^f}{\Delta\epsilon_{aibj} - \omega^f} \sum_Q \bar{B}^Q_{ai}[R^f] \hat{B}^Q_{bj} \Big). \tag{32}$$

The definitions of the intermediates $\hat{K}^{Q,m}$, $\bar{K}^{Q,m}$, $\bar{K}^{Q,m,x}$, and $\bar{\bar{K}}^{Q,m,x}$ are given in Table I.

### D. Evaluation of the relaxed densities

In Eq. (8) we expressed the contributions that depend on first derivatives of the MO integrals and the first derivative of the cluster amplitudes, $t^y$, or the right eigenvector, $R^{f,y}$, through derivatives of one- and two-particle densities. At this point we account for the fact that RI-CC2 can be combined with Hartree-Fock calculations that may or may not use the RI-JK approximation for ERIs[34] by splitting these contributions into a one-particle density which is contracted with derivatives of the Fock matrix—computed within the corresponding approximation used at the Hartree-Fock level—and a non-separable two-particle density which is always contracted with first derivatives of the ERIs in the RI approximation:

$$\sum_{pq} D^{F,ex,y}_{pq} F^x_{pq} + \frac{1}{2} \sum_{pqrs} \hat{d}^{ex,nsep,y}_{pqrs} \hat{P}^{pq}_{rs} \Big( \sum_Q \hat{B}^{Q,x}_{pq} \hat{B}^Q_{rs} \Big). \tag{33}$$

For a one-electron perturbation which does not change the AO basis the first derivative of the three-index integrals $\hat{B}^{Q,x}_{pq}$ is given by[29]

$$\hat{B}^{Q,x}_{pq} = \sum_r \Big( \kappa^x_{pr} \hat{B}^Q_{rq} + \kappa^x_{qr} \hat{B}^Q_{pr} \Big). \tag{34}$$

The one-electron density $D^{F,ex,y}_{pq}$ is given by

$$D^{F,ex,y}_{pq} = D^{F,A}_{pq}(\bar{t}^{f,(0)}, t^y) + D^{F,A}_{pq}(L^{f,(0)}, R^{f,y}) \tag{35}$$

TABLE I. Definition of the intermediates used in Eqs. (31) and (32). In the unrelaxed case $F^x_{pq}$ is replaced by the integrals for the perturbation operator in the similarity-transformed MO basis, $\hat{h}^x_{pq}$.

| |
|---|
| $\hat{K}^{Q,m}_{ai} = \hat{B}^Q_{ai} e^{-(\epsilon_a-\epsilon_i)\theta_m}$ |
| $\bar{K}^{Q,m}_{ai} = \bar{B}^Q_{ai} e^{-(\epsilon_a-\epsilon_i-\omega)\theta_m}$ |
| $\bar{\bar{K}}^{Q,m,x}_{ai} = \sum_b \hat{K}^{Q,m}_{bi} F^x_{ab} - \sum_k \hat{K}^{Q,m}_{ak} F^x_{ki}$ |
| $\bar{\bar{K}}^{Q,m,x}_{ai} = \sum_b \bar{K}^{Q,m}_{bi} F^x_{ab} - \sum_k \bar{K}^{Q,m}_{ak} F^x_{ki}$ |

and in a similar way the non-separable two-electron density is defined as

$$\hat{d}^{nsep,ex,y}_{pqrs} = \langle \mathrm{HF}|[[\hat{e}_{pqrs}, \hat{T}_1], \hat{T}^y_1] + [\hat{e}_{pqrs}, \hat{T}^y_2]|\mathrm{HF}\rangle + \hat{d}^{nsep,A}_{pqrs}(\bar{t}^{f,(0)}, t^y) + \hat{d}^{nsep,A}_{pqrs}(L^{f,(0)}, R^{f,y}) + \hat{d}^{nsep,B}_{pqrs}(L^{f,(0)}, R^{f,(0)}, t^y). \tag{36}$$

The first contributions given in second quantization are identical with density contributions described in Ref. 29 and the $A$ densities have been described in detail in Ref. 22. A qualitatively new density contribution for excited state second order properties is $\hat{d}^{nsep,B}_{pqrs}(L^{f,(0)}, R^{f,(0)}, t^y)$, which is related to the derivative of the Jacobi matrix with respect to the cluster amplitudes,

$$\hat{d}^{nsep,B}_{pqrs}(L^f, R^f, t^y) = \sum_{\mu_1} L^f_{\mu_1} \langle \mu_1 | [[\hat{e}_{pqrs}, \hat{T}^y_1 + \hat{T}^y_2], R^f_1] + [[\hat{e}_{pqrs}, \hat{T}^y_1], R^f_2]|\mathrm{HF}\rangle + \sum_{\mu_2} L^f_{\mu_2} \langle \mu_2 | [[\hat{e}_{pqrs}, \hat{T}^y_1], R^f_1]|\mathrm{HF}\rangle. \tag{37}$$

In the relaxed case, we exploit that the reference wave function fulfills the Brillouin condition and thus the occupied/virtual block of the Fock matrix, which would be contracted with the only non-zero elements of the corresponding one-electron density $D^{F,B}_{pq}(L^{f,(0)}, R^{f,(0)}, t^y)$, vanishes. The ERIs in Eq. (33) are one-index transformed with the orbital rotation parameter $\kappa^x$. To avoid $O(N^5)$-scaling steps for every pair of perturbations, the two-electron term in Eq. (33) is rewritten as

$$\frac{1}{2} \sum_{pqrs} \hat{d}^{ex,nsep,y}_{pqrs} \hat{P}^{pq}_{rs} \Big( \sum_Q \hat{B}^{Q,x}_{pq} \hat{B}^Q_{rs} \Big) = \sum_{pq} F^{eff,y}_{pq} \kappa^x_{pq} \tag{38}$$

with the effective Fock matrices

$$F^{eff,y}_{pq} = \sum_{rst} (\hat{d}^{ex,nsep,y}_{rstp} + \hat{d}^{ex,nsep,y}_{rspt}) (rs|tq)^{RI}. \tag{39}$$

The effective Fock matrices in the last equation are similar to those used for ground state polarizabilities, but are computed with different densities.[22,29,35] Explicit expressions for the two-electron B density, Eq. (37), and the effective Fock

This article is copyrighted as indicated in the article. Reuse of AIP content is subject to the terms at: http://scitation.aip.org/termsconditions. Downloaded to IP: 134.147.252.238 On: Thu, 14 Jan 2016 14:18:42

matrices, Eq. (39), are given for the interested reader in the supplementary material.[25]

In the unrelaxed case, the two-electron contribution vanishes for a pure one-electron perturbation. The one-electron density is in the unrelaxed case contracted with the first derivatives of the one-electron integrals $\hat{h}^x_{pq}$ in the $\Lambda^p, \Lambda^h$-basis (cmp. Eq. (10)). In addition, the expressions for the densities are slightly different because of the differences in the doubles equations,

$$\hat{D}^{ex,ur}_{pq} = \langle \mathrm{HF}|[\hat{E}_{pq}, \hat{T}^y_1]|\mathrm{HF}\rangle + \hat{D}^A_{pq}(\bar{t}^{f,(0)}, t^y) + \hat{D}^A_{pq}(L^{f,(0)}, R^{f,y}) + \hat{D}^B_{pq}(L^{f,(0)}, t^y, R^{f,(0)}) \quad (40)$$

with

$$\hat{D}^B_{pq}(L^{f,(0)}, t^y, R^{f,(0)}) = \sum_{\mu_1} L^f_{\mu_1}\langle \mu_1|[[\hat{E}_{pq}, \hat{T}^y_1], R^f_1]|\mathrm{HF}\rangle + \sum_{\mu_2} L^f_{\mu_2}\langle \mu_2|[[\hat{E}_{pq}, R^f_1], \hat{T}^y_2] + [[\hat{E}_{pq}, \hat{T}^y_1], R^f_2]|\mathrm{HF}\rangle. \quad (41)$$

Details for the unrelaxed one-electron density $\hat{D}^A$ have been given in Ref. 32.

### E. One-index transformed excited state density

The orbital-relaxed case requires the evaluation of the expectation value for the effective second-order Hamiltonian,[26]

$$\hat{J}^{xy} = \hat{P}^{xy}[\hat{\kappa}^x, \hat{h}^y] + \frac{1}{2}\hat{P}^{xy}[\hat{\kappa}^x, [\hat{\kappa}^y, \hat{H}]] = \hat{P}^{xy}[\hat{\kappa}^x, \hat{\mathcal{J}}^y], \quad (42)$$

with the modified effective first-order Hamiltonian $\hat{\mathcal{J}}^y = \hat{h}^y + \frac{1}{2}[\hat{\kappa}^y, \hat{H}]$.[29] The computation of doubly one-index transformed two-electron integrals would introduce costs that scale as $O(\mathcal{N}^5)$ with the system size and with the number of pairs of perturbations. To avoid this, the expectation value of $\hat{J}^{xy}$ is expressed as a contraction of orbital rotation parameters with effective Fock matrices,

$$\langle \hat{J}^{xy}\rangle^{ex} = \hat{P}^{xy}\sum_{pq}\kappa^y_{pq}F^{eff}_{pq}[\hat{\mathcal{J}}^x] \quad (43)$$

with $F^{eff}_{pq}[\hat{\mathcal{J}}^x]$ evaluated as

$$F^{eff}_{pq}[\hat{\mathcal{J}}^x] = \sum_t\left(D^{eff}_{pt}F_{qt}[\hat{\mathcal{J}}^x] + D^{eff}_{tp}F_{tq}[\hat{\mathcal{J}}^x]\right) + \frac{\nu_p}{4}\left(G\{D^{corr}\}^x_{qp} + G\{D^{corr}\}^x_{pq}\right) + \sum_{Qt}\left(\Delta^{ex,Q}_{pt}\hat{B}^{Q,x}_{qt} + \Delta^{ex,Q,x}_{pt}\hat{B}^Q_{qt} + \Delta^{ex,Q}_{tp}\hat{B}^{Q,x}_{tq} + \Delta^{ex,Q,x}_{tp}\hat{B}^Q_{tq}\right). \quad (44)$$

$\nu_p$ are the SCF occupation numbers. The definition of the other intermediates can be found in Table II. The effective Fock matrix is calculated in a similar way as for the ground state (comp. Refs. 29 and 35), but with the excited state instead of the ground state one- and two-electron densities.

The approach described above to compute excited state polarizabilities with CC2 or related approximations has been implemented in a development version of the TURBOMOLE program package.[36]

## III. RESULTS

### A. Thresholds and numerical accuracy

A measure for the accuracy of the numerical Laplace transformation is the error function

$$F^{Lap}(\theta_m, w_m) = \int_{\epsilon_{min}}^{\epsilon_{max}}\left(\frac{1}{x} - \sum_m^{N_m} w_m e^{-x\theta_m}\right)^2 dx, \quad (45)$$

which is minimized to determine the Laplace grid points $\theta_m$ and weights $w_m$. $\epsilon_{max}$ and $\epsilon_{min}$ are, respectively, the maximum and minimum orbital energy denominators, shifted by an excitation or external field frequency. Beside $F^{Lap}$, the accuracy of the excited state polarizabilities depends also on the convergence of the eigenvalue problem for the excitation energies and eigenvectors and the convergence of the linear response equations for the Lagrange multipliers and the first derivatives of the cluster amplitudes and right eigenvectors which are controlled via two thresholds, $T_{Eig}$ and $T_{LRE}$ as

$$\|(\mathbf{A}^{eff} - \omega^f)R^f\| \le T_{Eig}, \quad (46)$$

$$\|(\mathbf{A}^{eff} - \omega_x)t^x - \xi^{eff,x}\| \le T_{LRE}. \quad (47)$$

To study the dependence of the excited state polarizabilities on the different convergence criteria, the orbital-unrelaxed excited state polarizability has been calculated with CC2 and the aug-cc-pVDZ[37,38] basis set for 16 different states in the five molecules benzene, water, formaldehyde, ethene, naphthalene. The frozen core approximations have been used throughout this work for the 1*s* electrons at C and O. The thresholds for the Laplace transformation and the response equations were varied independently while the threshold for the eigenvalue equations was set to $0.01 \times T_{LRE}$. This is sufficient for excited states which are energetically well separated. Nearly degenerated states require tighter values for $T_{eig}$ to get converged results for the polarizabilities. The reference values were taken from

TABLE II. Definition of the intermediates used in Eq. (44). The formulas for the three-index integrals $\hat{B}^Q_{rs}$ and $\hat{B}^{Q,x}_{rs}$ are given in the supplementary material,[25] the definition of the densities have been given in Ref. 22.

| |
|---|
| $F_{tq}[\hat{\mathcal{J}}^x] = \frac{1}{2}F_{tq}[\{\hat{\kappa}^x, \hat{H}\}] + h^x_{tq}$ |
| $F_{tq}[\{\hat{\kappa}^x, \hat{H}\}] = \{\hat{\kappa}^x, h\}_{tq} + \frac{1}{4}\sum_{rs}D^{\mathrm{SCF}}_{rs}\{\hat{\kappa}^x, A\}_{pqrs}$ |
| $A_{pqrs} = 4(pq\|rs) - (pr\|sq) - (ps\|rq)$ |
| $G\{D^{corr}\}^x_{pq} = \sum_{rs}\frac{1}{4}D^{corr}_{rs}\{\hat{\kappa}^x, A\}_{pqrs}$ |
| $D^{eff}_{pq} = D^{corr}_{pq} + D^{\mathrm{SCF}}_{pq}$ |
| $D^{corr}_{pq} = D^{F,A}_{pq} + D^{F,\xi}_{pq} + \frac{1}{2}(\bar{\kappa}_{pq} + \bar{\kappa}_{qp})$ |
| $\Delta^{ex,Q}_{pt} = \sum_{rs}\hat{d}^{nsep,ex}_{ptrs}\hat{B}^Q_{rs}$ |
| $\Delta^{ex,Q,x}_{pt} = \sum_{rs}\hat{d}^{nsep,ex}_{ptrs}\hat{B}^{Q,x}_{rs}$ |
| $\hat{d}^{nsep,ex}_{pqrs} = \hat{d}^{nsep,A}_{pqrs} + \hat{d}^{nsep,\xi}_{pqrs}$ |

This article is copyrighted as indicated in the article. Reuse of AIP content is subject to the terms at: http://scitation.aip.org/termsconditions. Downloaded to IP: 134.147.252.238 On: Thu, 14 Jan 2016 14:18:42

tightly converged calculations with $\sqrt{F^{Lap}}$ and $T_{LRE}$ set to $\leq 10^{-10}$. For every state, we evaluated the maximum relative error in a diagonal tensor component,

$$\Delta\alpha_{max} = \max\left(\frac{\alpha_{ii} - \alpha_{ii}^{ref}}{\alpha_{ii}^{ref}}\right) \text{with } i \in \{x, y, z\}. \quad (48)$$

Figure 1 shows the results for the $2\,^1B_2$ state of formaldehyde. Even with the loosest threshold for the Laplace transformation the relative error is below 1%. With increasing number of grid points the error follows a power law $c \times F_{Lap}^{b}$ or the curves flatten out. In the latter case, the relative error is dominated by the incomplete convergence of the response equations. Similar figures were obtained for the remaining test cases (see supplementary material[25]). From these results, we obtained as an estimate for the upper bound of the relative errors,

$$\Delta\alpha_{max} \leq 0.1\sqrt{F^{Lap}} + T_{LRE}. \quad (49)$$

### B. Comparison with experimental data

To test the accuracy of CC2 in predicting excited state polarizabilities, the change of the isotropic excited state polarizability was calculated for 18 different states in 13 molecules as $\Delta\bar{\alpha} = \frac{1}{3}\mathrm{Tr}(\alpha^{ex}) - \frac{1}{3}\mathrm{Tr}(\alpha^{gs})$, where $\alpha^{ex}$ is the polarizability of the excited and $\alpha^{gs}$ the polarizability of the ground state. The structures for the ground and the excited state have been optimized with CC2 and the aug-cc-pVTZ basis[37,38] together with the corresponding optimized auxiliary basis set.[39] An exception was made for octacene, nanocene, and decacene, for which the structures have only been optimized with a cc-pVTZ basis set.[37,39] All polarizabilities have been calculated with the aug-cc-pVTZ basis set.[37–39]

The results for orbital-relaxed and unrelaxed CC2 are summarized in Table III. Stark spectroscopy measurements of jet cooled molecules in the gas phase are listed as the experimental reference for the first excited states of benzene, naphthalene, and anthracene.[40–42] The polarizability of the second excited state of naphthalene was determined from Stark effect measurements in solution,[43] whereas the molecules tetracene and pentacene were measured in doped crystals.[44,45]

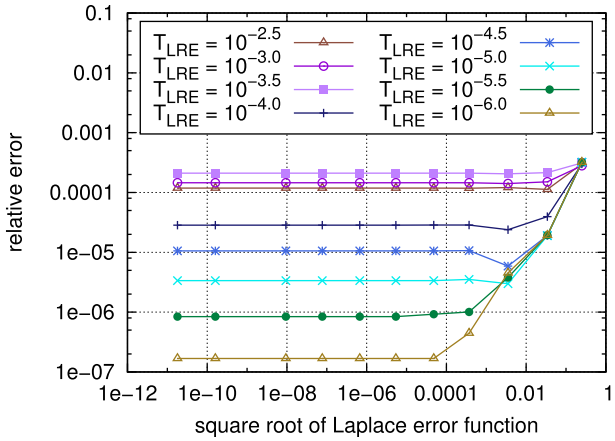



FIG. 1. $\Delta\alpha_{max}$ for the $2\,^1B_2$ state in formaldehyde as a function of $\sqrt{F^{Lap}}$ and the threshold for the linear response equations $T_{LRE}$.

TABLE III. Comparison of the calculated and experimental isotropic excited state polarizability changes. All values are given in atomic units. The mean deviation (MD), the mean absolute deviation (MAD), and the standard deviation (STDEV) to the experimental values are given. The deviation refers to the total calculated polarizability and is calculated as $^{(\Delta\bar{\alpha}^{calc} - \Delta\bar{\alpha}^{exp})}/_{\bar{\alpha}^{calc}}$.

| | | | CC2 | | | |
|---|---|---|---|---|---|---|
| | Symmetry | State | Relaxed | Unrelaxed | Expt. | Reference |
| Benzene | $D_{6h}$ | $1^1B_{2u}$ | 2 | 3 | 6 | 40 |
| Naphthalene | $D_{2h}$ | $1^1B_{2u}$ | 10 | 15 | 11 | 41 |
| | | $1^1B_{1u}$ | 73 | 96 | 66 | 43 |
| Anthracene | $D_{2h}$ | $1^1B_{1u}$ | 111 | 145 | 123 | 42 |
| Tetracene | $D_{2h}$ | $1^1B_{1u}$ | 178 | 233 | 180 | 44 |
| Pentacene | $D_{2h}$ | $1^1B_{1u}$ | 285 | 370 | 295 | 45 |
| Toluene | $C_S$ | $1^1A''$ | 6 | 8 | 18 | 46 |
| Phenanthrene | $C_{2v}$ | $1^1A_1$ | 39 | 56 | 34 | 46 |
| | | $1^1B_2$ | 133 | 172 | 117 | 46 |
| | | $3^1B_2$ | 163 | 230 | 172 | 46 |
| Chrysene | $C_{2h}$ | $1^1B_u$ | 59 | 80 | 51 | 46 |
| Picene | $C_{2v}$ | $1^1A_1$ | 111 | 149 | 66 | 46 |
| Pyrene | $D_{2h}$ | $1^1B_{1u}$ | 19 | 31 | 32 | 46 |
| Coronene | $C_{2h}$ | $1^1A_u$ | 38 | 63 | 33 | 46 |
| | | $1^1B_u$ | 129 | 193 | 123 | 46 |
| Carbazol | $C_{2v}$ | $1^1A_1$ | 68 | 88 | 47 | 46 |
| | | $1^1B_2$ | 81 | 102 | 63 | 46 |
| m-Nitroanilin | $C_1$ | $2^1A$ | 52 | 63 | 65 | 46 |
| MD | | | 0% | 8% | | |
| MAD | | | 5% | 10% | | |
| STDEV | | | 6% | 8% | | |

The remaining excited state polarizabilities were determined in solution using the spectral solvent-shift method.[46] The assignment of the irreducible representation of the excited state follows the conventions of Ref. 47.

As already known from the results for ground state polarizabilities,[29] unrelaxed CC2 tends to overestimate the polarizability. This applies also to the polarizability in excited states and the change of the polarizability upon excitation. Compared to relaxed CC2, unrelaxed CC2 values are about 10% larger in most cases. The error of unrelaxed CC2 to the experimental value is mostly around 10% and is in the test set largest for the first excited $^1A_1$ state in picene with 18%.

If one focuses on the molecules measured in the gas phase, there is a good agreement between the excited state polarizability calculated with orbital-relaxed CC2 and the experimental values measured for benzene, the $1\,^1B_{2u}$ state in naphthalene and anthracene. The maximum error for these three molecules is 6% for benzene. The calculated values for the change of the polarizability upon excitation for tetracene and pentacene are also close to the experimental values and in line with this finding. From the 13 states measured in solution, six molecules have an error below 5% and five an error below or equal 10%. A larger error is found for the $1\,^1A''$ state of toluene and the $1\,^1A_1$ state of picene, which have errors of 13% and 11%, respectively. Beside these two states, the agreement between experimental and calculated values is reasonable.

In Table III also the mean deviation, the mean absolute deviation, and the standard deviation are given. However, due to rather large experimental errors and solvent and crystal field

This article is copyrighted as indicated in the article. Reuse of AIP content is subject to the terms at: http://scitation.aip.org/termsconditions. Downloaded to IP: 134.147.252.238 On: Thu, 14 Jan 2016 14:18:42

effects the transferability of these results to other examples is limited. Nevertheless, with a mean absolute deviation of 5% orbital relaxed CC2 seems to be able to predict excited state polarizabilities and is more appropriate than unrelaxed CC2 with a mean absolute deviation of 10%. A larger data set of accurately determined experimental data would be required for a more reliable test set.

For the polyacenes up to pentacene, there are experimental values available for the changes in the three individual components of the polarizability tensor upon excitation. In Table IV, these values are listed together with the orbital-relaxed CC2 results. The molecules are orientated with the $y$ and the $z$ axis in the molecular plane and the $x$ axis perpendicular to it. The $y$ axis is oriented along the long molecular axis. Except for the $x$ component of benzene, there is a reasonable agreement of the calculated polarizability components of benzene and naphthalene with the experimental data. For the other molecules the agreement between the calculated and the experimental results is poor. In particular, for the $x$ component, the calculated change in the polarizability upon excitation is small and nearly constant around 2 a.u. for all molecules, whereas the experimental values for this component decrease between anthracene and pentacene from +52 to −128 a.u. However, it should be mentioned that the small change in the $x$ component is more in line with what is expected from the physical intuition for these systems. For the $z$ component, the calculated values increase only slowly, while there is a much faster increase in the experimental data from anthracene to pentacene. In contrast to this, the theoretical and experimental results for the $y$ component increase, in line with each other, with the number of benzene units. However, beyond anthracene the computed CC2 results increase faster with the chain length than the experimental values. It is difficult to judge to which extent the deviations between the computed gas phase values and the experimental results, with tetracene and pentacene measured in doped crystals, are due to the remaining errors of the electronic structure method. For tetracene and pentacene, further crystal field effects may play a role.

TABLE IV. Components of the excited state polarizability change for the lowest excited states of some polyacenes ($1\,^1B_{2u}$ for benzene and naphthalene, $1\,^1B_{1u}$ for the other polyacenes). The calculated results have been obtained with relaxed CC2/aug-cc-pVTZ. All values are given in atomic units.

| | $\Delta\alpha_{xx}$ | | $\Delta\alpha_{yy}$ | | $\Delta\alpha_{zz}$ | | |
|---|---|---|---|---|---|---|---|
| | Calc. | Expt. | Calc. | Expt. | Calc. | Expt. | Reference |
| Benzene | 6 | 15 | 0 | 2 | 0 | 2 | 40 |
| Naphthalene | 4 | 6 | 27 | 25 | −2 | 1 | 41 |
| Anthracene | 5 | 52 | 307 | 338 | 20 | −18 | 42 |
| Tetracene | 3 | −54 | 513 | 439 | 18 | 155 | 44 |
| Pentacene | 2 | −128 | 829 | 587 | 22 | 425 | 45 |
| Hexacene | 2 | | 1285 | | 33 | | |
| Heptacene | 2 | | 1921 | | 48 | | |
| Octacene | 2 | | 2729 | | 61 | | |
| Nanocene | 2 | | 3776 | | 58 | | |
| Decacene | 2 | | 5060 | | 17 | | |

Table V shows a comparison between CC2, CIS($D_\infty$), and CCS for isotropically averaged excited state polarizabilities. For CC2 and CCS, both orbital-relaxed and unrelaxed results are listed. Note that in the orbital-relaxed case CCS is equivalent to Hartree-Fock for the ground state and to configuration interaction singles (CIS) in the excited state. The CIS($D_\infty$) excited state polarizabilities are close to the relaxed CC2 values. The deviation between these two methods is mostly around 1%. However, larger differences can be found for nanocene and decacene where the deviations are 7% and 12%, respectively. Also for the $2\,^1A$ state of *meta*-nitroanilin, the deviation is with 11% relatively large. Compared to CIS($D_\infty$), the deviations between CCS and CC2 are much larger, irrespective of the inclusion of orbital relaxation. The mean absolute deviation between the relaxed and unrelaxed CCS values and the orbital-relaxed CC2 reference results is about 20%. Larger deviations of about 40% are observed for the longer polyacenes. The large deviations between CC2 and CCS for the larger polyacenes might be related to the increasing contribution of doubly excited configurations to the excited state. In many cases, the relaxed CCS results are smaller than the CC2 results. The unrelaxed CCS results are larger than the relaxed CCS results and thus usually closer to the CC2 results.

TABLE V. Isotropic average of the excited state polarizabilities calculated with CC2, CIS($D_\infty$), and CCS. All values are given in atomic units. The mean deviation (MD), the mean absolute deviation (MAD), and the standard deviation (STDEV) refer to the relative deviations from the orbital-relaxed CC2 values.

| | Symmetry, State | CC2 relaxed | CC2 unrelaxed | CIS($D_\infty$) relaxed | CCS relaxed | CCS unrelaxed |
|---|---|---|---|---|---|---|
| Benzene | $D_{6h}$, $1\,^1B_{2u}$ | 71 | 75 | 71 | 82 | 90 |
| Naphthalene | $D_{2h}$, $1\,^1B_{2u}$ | 131 | 140 | 130 | 138 | 152 |
| | $1\,^1B_{1u}$ | 195 | 222 | 193 | 150 | 163 |
| Anthracene | $D_{2h}$, $1\,^1B_{1u}$ | 294 | 336 | 291 | 232 | 254 |
| Tetracene | $D_{2h}$, $1\,^1B_{1u}$ | 436 | 503 | 431 | 332 | 364 |
| Pentacene | $D_{2h}$, $1\,^1B_{1u}$ | 627 | 729 | 622 | 454 | 496 |
| Hexacene | $D_{2h}$, $1\,^1B_{1u}$ | 876 | 1024 | 875 | 599 | 649 |
| Heptacene | $D_{2h}$, $1\,^1B_{1u}$ | 1196 | 1402 | 1209 | 769 | 825 |
| Octacene | $D_{2h}$, $1\,^1B_{1u}$ | 1577 | 1851 | 1630 | 959 | 1017 |
| Nanocene | $D_{2h}$, $1\,^1B_{1u}$ | 2041 | 2399 | 2181 | 1178 | 1231 |
| Decacene | $D_{2h}$, $1\,^1B_{1u}$ | 2578 | 3036 | 2892 | 1427 | 1461 |
| Toluene | $C_s$, $1\,^1A''$ | 89 | 93 | 89 | 102 | 112 |
| Phenanthrene | $C_{2v}$, $1\,^1A_1$ | 214 | 238 | 214 | 210 | 233 |
| | $1\,^1B_2$ | 308 | 354 | 302 | 209 | 227 |
| | $3\,^1B_2$ | 338 | 412 | 324 | 266 | 297 |
| Chrysene | $C_{2h}$, $1\,^1B_u$ | 294 | 325 | 293 | 280[a] | 308[a] |
| Picene | $C_{2v}$, $1\,^1A_1$ | 411 | 461 | 410 | 363 | 398 |
| Pyrene | $D_{2h}$, $1\,^1B_{1u}$ | 221 | 243 | 219 | 221 | 244 |
| Coronene | $C_{2h}$, $1\,^1A_u$ | 350 | 391 | 349 | 326 | 362 |
| | $1\,^1B_u$ | 441 | 522 | 438 | 332 | 365 |
| Carbazol | $C_{2v}$, $1\,^1A_1$ | 226 | 252 | 224 | 217 | 241 |
| | $1\,^1B_2$ | 239 | 267 | 237 | 211 | 231 |
| m-Nitroanilin | $C_1$, $2\,^1A$ | 154 | 169 | 170 | 128 | 143 |
| MD | | | 13% | 1% | −17% | −9% |
| MAD | | | 13% | 2% | 20% | 18% |
| STDEV | | | 4% | 4% | 17% | 20% |

[a]Values for the $2\,^1B_u$ state, which corresponds to the $1\,^1B_u$ state of CC2.

This article is copyrighted as indicated in the article. Reuse of AIP content is subject to the terms at: http://scitation.aip.org/termsconditions. Downloaded to IP: 134.147.252.238 On: Thu, 14 Jan 2016 14:18:42

TABLE VI. Isotropic average of the excited state polarizabilities calculated with CC2, CIS($D_\infty$), and CCS at the relaxed excited state geometry. All values are given in atomic units.

| | Symmetry, State | CC2 relaxed | CC2 unrelaxed | CIS($D_\infty$) relaxed | CCS relaxed | CCS unrelaxed |
|---|---|---|---|---|---|---|
| Benzene | $D_{6h}, 1^1B_{2u}$ | 72 | 76 | 72 | 84 | 92 |
| Naphthalene | $D_{2h}, 1^1B_{2u}$ | 131 | 140 | 130 | 139 | 153 |
| | $D_{2h}, 1^1B_{1u}$ | 182 | 205 | 181 | 150 | 163 |
| Anthracene | $D_{2h}, 1^1B_{1u}$ | 285 | 324 | 284 | 233 | 254 |
| Tetracene | $D_{2h}, 1^1B_{1u}$ | 428 | 490 | 428 | 334 | 364 |
| Pentacene | $D_{2h}, 1^1B_{1u}$ | 619 | 717 | 626 | 458 | 497 |
| Toluene | $C_s, 1^1A''$ | 89 | 94 | 89 | 102 | 112 |
| Phenanthrene | $C_{2v}, 1^1A_1$ | 214 | 238 | 213 | 211 | 233 |
| | $1^1B_2$ | 292 | 334 | 287 | 219 | 236 |
| | $3^1B_2$ | 281 | 331 | 270 | 238 | 264 |
| Chrysene | $C_{2h}, 1^1B_u$ | 293 | 324 | 291 | 282[a] | 310[a] |
| Picene | $C_{2v}, 1^1A_1$ | 411 | 463 | 409 | 368 | 404 |
| Pyrene | $D_{2h}, 1^1B_{1u}$ | 220 | 241 | 217 | 223 | 246 |
| Coronene | $C_{2h}, 1^1A_u$ | 348 | 389 | 347 | 329 | 365 |
| | $1^1B_u$ | 437 | 515 | 433 | 338 | 370 |
| Carbazol | $C_{2v}, 1^1A_1$ | 223 | 248 | 221 | 190 | 212 |
| | $1^1B_2$ | 232 | 261 | 230 | 209 | 228 |
| m-Nitroanilin | $C_1, 2^1$ A | 136 | 148 | 133 | 122 | 136 |

[a]Values for the $2^1B_u$ state, which corresponds to the $1^1B_u$ state of CC2.

So far, all values were computed at the ground state structures. For a subset of the molecules, we computed also the polarizabilities at the equilibrium geometry of the excited state. The results are compiled in Table VI. In most cases, the equilibrium geometry in the excited state is close to the ground state structure and then the differences in the polarizabilities at the two structures are small. Except for benzene, where the polarizability increases slightly with 1%, the excited state polarizabilities in general decrease upon relaxation of the structure by about 3%. A special case is the $3\,^1B_2$ state of phenanthrene. Here, the molecule adopts in the excited state a slightly twisted structure with a lower symmetry than the ground state geometry. In this case, the excited state polarizability decreases by 17%. Applying unrelaxed CC2, the decrease in the excited state polarizabilities is marginally stronger compared to the relaxed values. The CIS($D_\infty$) results are again close to the relaxed CC2 results. For CCS the differences in the polarizabilities between the two structures are still small. However, one observes more frequently a small increase from the ground to the excited state equilibrium geometry.

### C. Computational Performance

Table VII summarizes timings for CC2 and CIS($D_\infty$) calculations on the polyacenes with 6–10 annulated rings. The timings demonstrate that even for large systems as decacene with almost 2500 basis functions, excited state polarizabilities can be obtained within about 4 days on just one compute node with 12 CPU cores. The overall timings are dominated by non-iterative steps, in particular the computation of the densities. Therefore, CIS($D_\infty$) is only about 20% faster than orbital-relaxed CC2. The orbital-unrelaxed version of CC2 is about 30% faster than its relaxed counterpart, but also overestimates the polarizabilities. Compared to the ground state polarizabilities (see Ref. 29), the computation of excited state polarizabilities takes approximately twice as much time.

## IV. CONCLUSION

Excited state polarizabilities have been implemented for CC2 and CIS($D_\infty$) as the second derivative of an excited state quasienergy Lagrangian. By using appropriate constraints for the norm and phase of the eigenvectors secular divergent terms are avoided. The resulting response equations are numerically stable in the limit of frequency-independent perturbations, but involve a Jacobian matrix which is projected onto the orthogonal complemented of the unperturbed eigenvectors. We devise an algorithm how these equations can be solved efficiently without storing the double excitation parts of any coefficient vectors.

To achieve an implementation which can be applied to large molecules, care has been taken to limit the scaling of main memory demands with the system size to $O(N^2)$ and the scaling of the disc storage demands to $O(N^3)$. This could be realized by combining the RI approximation with a numerical Laplace transformation of orbital energy denominators for the calculation of the correlation contribution to some one-electron densities. Both approximations enable calculations on molecules as large as decacene with nearly 2500 basis functions within 4 days on 12 CPU cores with an OpenMP parallelization.

The orbital-relaxed CC2 results for isotropic excited state polarizabilities agree well, usually within 5%, with the experimental reference results where gas phase measurements are available. Unrelaxed CC2 tends to overestimate the polarizability in excited states similarly as in the ground state. The unrelaxed CC2 results are on average 10%–15% larger than their orbital-relaxed counterparts. However,

TABLE VII. Timings for calculations of larger molecules. The calculations were performed on 12 cores of 2 Intel(R) Xenon(R) X5670 CPUs with 2.93 GHz.

| | No. basis function | | Wall clock time / h | | |
|---|---|---|---|---|---|
| | MO | Auxiliary | CC2, relaxed | CC2, unrelaxed | CIS($D_\infty$), relaxed |
| Hexacene | 1564 | 3492 | 11 | 7 | 8 |
| Heptacene | 1794 | 4008 | 19 | 12 | 15 |
| Octacene | 2024 | 4524 | 34 | 25 | 26 |
| Nanocene | 2254 | 5040 | 55 | 39 | 43 |
| Decacene | 2484 | 5556 | 85 | 62 | 65 |

This article is copyrighted as indicated in the article. Reuse of AIP content is subject to the terms at: http://scitation.aip.org/termsconditions. Downloaded to IP: 134.147.252.238 On: Thu, 14 Jan 2016 14:18:42

only the unrelaxed approach has a physically consistent pole structure for frequency-dependent polarizabilities. The CIS($D_\infty$) approximation gives, in the orbital-relaxed case, results which are within a few percent of the CC2 results, but is also only 20% faster than CC2 since the computation time for excited state second-order properties is dominated by non-iterative steps which are almost the same for CIS($D_\infty$) and CC2.

The implementation of excited state polarizabilities is also a keystone for a forthcoming implementation of dipole gradients and force constants.

## ACKNOWLEDGMENTS

We gratefully acknowledge financial support by the Deutsche Forschungsgemeinschaft (DFG) through grant no. HA 2588/5 and the Cluster of Excellence RESOLV (EXC 1069).

[1]M. Ponder and R. Mathies, J. Phys. Chem. **87**, 5090 (1983).
[2]O. Christiansen, H. Koch, and P. Jørgensen, Chem. Phys. Lett. **243**, 409 (1995).
[3]C. Hättig, Adv. Quantum Chem. **50**, 37 (2005).
[4]M. Schütz, J. Hutter, and H. P. Lüthi, J. Chem. Phys. **103**, 7048 (1995).
[5]J. F. Stanton and J. Gauss, J. Chem. Phys. **104**, 9859 (1996).
[6]C. Hättig, O. Christiansen, S. Coriani, and P. Jørgensen, J. Chem. Phys. **109**, 9237 (1998).
[7]S. Heitz, D. Weidauer, and A. Hese, J. Chem. Phys. **95**, 7952 (1991).
[8]F. C. Grozema, R. Telesca, H. T. Jonkman, L. D. A. Siebbeles, and J. G. Snijders, J. Chem. Phys. **115**, 10014 (2001).
[9]T. Pluta, M. Kolaski, M. Medved', and Š Budzák, Chem. Phys. Lett. **546**, 24 (2012).
[10]P. Norman, D. Jonsson, O. Vahtras, and H. Ågren, Chem. Phys. **203**, 23 (1996).
[11]D. Jonsson, P. Norman, and H. Ågren, J. Chem. Phys. **105**, 6401 (1996).
[12]D. Jonsson, P. Norman, and H. Ågren, Chem. Phys. **224**, 201 (1997).
[13]B. Jansik, D. Jonsson, P. Sałek, and H. Ågren, J. Chem. Phys. **121**, 7595 (2004).
[14]J. F. Stanton and J. Gauss, J. Chem. Phys. **103**, 8931 (1995).
[15]C. Hättig and P. Jørgensen, J. Chem. Phys. **109**, 9219 (1998).
[16]O. Christiansen, C. Hättig, and P. Jørgensen, Spectrochim. Acta, Part A **55**, 509 (1999).
[17]J. L. Whitten, J. Chem. Phys. **58**, 4496 (1973).
[18]B. I. Dunlap, J. W. D. Connolly, and J. R. Sabin, J. Chem. Phys. **71**, 3396 (1979).
[19]O. Vahtras, J. Almlöf, and M. Feyereisen, Chem. Phys. Lett. **213**, 514 (1993).
[20]C. Hättig and F. Weigend, J. Chem. Phys. **113**, 5154 (2000).
[21]O. Christiansen, P. Jørgensen, and C. Hättig, Int. J. Quantum Chem. **68**, 1 (1998).
[22]A. Köhn and C. Hättig, J. Chem. Phys. **119**, 5021 (2003).
[23]T. Helgaker, P. Jørgensen, and J. Olsen, *Molecular Electronic Structure Theory* (Wiley, 2000).
[24]T. Helgaker and P. Jørgensen, Theor. Chim. Acta **75**, 111 (1989).
[25]See supplementary material at http://dx.doi.org/10.1063/1.4937944 for explicit working equations for right hand side vectors, two-particle densities, and effective fock matrices.
[26]T. Helgaker and P. Jørgensen, Adv. Quantum Chem. **19**, 183 (1988).
[27]H. Koch, O. Christiansen, R. Kobayashi, P. Jørgensen, and T. Helgaker, Chem. Phys. Lett. **228**, 233 (1994).
[28]O. Christiansen, C. Hättig, and J. Gauss, J. Chem. Phys. **109**, 4745 (1998).
[29]D. H. Friese, N. O. C. Winter, P. Balzerowski, R. Schwan, and C. Hättig, J. Chem. Phys. **136**, 174106 (2012).
[30]M. Head-Gordon, M. Oumi, and D. Maurice, Mol. Phys. **96**, 593 (1999).
[31]J. Schirmer, Phys. Rev. A **26**, 2395 (1982).
[32]C. Hättig and A. Köhn, J. Chem. Phys. **117**, 6939 (2002).
[33]J. Almlöf, Chem. Phys. Lett. **181**, 319 (1991).
[34]F. Weigend, Phys. Chem. Chem. Phys. **4**, 4285 (2002).
[35]D. H. Friese, C. Hättig, and J. Koßmann, J. Chem. Theory Comput. **9**, 1469 (2013).
[36]TURBOMOLE V7.0 2015, a development of University of Karlsruhe and Forschungszentrum Karlsruhe GmbH, 1989-2007, TURBOMOLE GmbH, since 2007, available from http://www.turbomole.com.
[37]T. H. Dunning, Jr., J. Chem. Phys. **90**, 1007 (1989).
[38]R. A. Kendall, T. H. Dunning, and R. J. Harrison, J. Chem. Phys. **96**, 6796 (1992).
[39]F. Weigend, A. Köhn, and C. Hättig, J. Chem. Phys. **116**, 3175 (2002).
[40]M. Okruss, R. Müller, and A. Hese, J. Chem. Phys. **110**, 10393 (1999).
[41]S. Heitz, D. Weidauer, B. Rosenow, and A. Hese, J. Chem. Phys. **96**, 976 (1992).
[42]V. Bendkowsky, E. Heinecke, and A. Hese, J. Chem. Phys. **127**, 224306 (2007).
[43]R. Mathies and A. C. Albrecht, J. Chem. Phys. **60**, 2500 (1974).
[44]J. Meyling, P. Bounds, and R. Munn, Chem. Phys. Lett. **51**, 234 (1977).
[45]E. Heinecke, Ph.D. thesis, Technische Universität Berlin, 1999.
[46]I. Renge, Chem. Phys. **167**, 173 (1992).
[47]R. S. Mulliken, J. Chem. Phys. **23**, 1997 (1955).

This article is copyrighted as indicated in the article. Reuse of AIP content is subject to the terms at: http://scitation.aip.org/termsconditions. Downloaded to IP: 134.147.252.238 On: Thu, 14 Jan 2016 14:18:42